HHS Public Access

Author manuscript

Antiviral Res. Author manuscript; available in PMC 2020 May 15.

Published in final edited form as:

Antiviral Res. 2018 August ; 156: 85–91. doi:10.1016/j.antiviral.2018.06.005.

Long-acting parenteral combination antiretroviral loaded nano-drug delivery system to treat chronic HIV-1 infection: A humanized mouse model study

Subhra Mandal[a,*], **Guobin Kang**[b], **Pavan Kumar Prathipati**[a], **Wenjin Fan**[b], **Qingsheng Li**[b], **Christopher J. Destache**[a,c]

[a]School of Pharmacy & Health Professions, Creighton University, Omaha, NE 68178, USA

[b]Center for Virology, University of Nebraska-Lincoln, 4240 Fair St, Lincoln, NE 68583, USA

[c]School of Medicine, Division of Infectious Diseases, Creighton University, Omaha, NE 68178, USA

Abstract

Human immunodeficiency virus (HIV) patients are often diagnosed in the chronic stage of HIV/AIDS. Combination antiretroviral therapy (cART) has improved quality of life for HIV-infected patients. Present study describes a novel long-acting parenteral formulation of combination antiretroviral (cARV) loaded nano-drugs for treating chronic HIV-1 (cHIV) in a humanized-BLT (hu-BLT) mice model. The cARV (elvitegravir + tenofovir alafenamide + emtricitabine; EVG + TAF + FTC) drugs (mimicking marketed Genvoy® one-pill for HIV-treatment) were encapsulated in poly (lactic-co-glycolic acid) nanoparticles (NPs). To establish cHIV, hu-BLT mice were intravaginally challenged with HIV-1 and maintained for 15 weeks. Plasma viral load (pVL) was monitored by RT-PCR to confirm cHIV. Baseline pVL (week 15) was comparable between treated (n = 10) and control (n = 5) mice groups. Subsequently, treatment hu-BLT mice received 3 subcutaneous doses of cARV NPs (417 mg/kg per dose; n = 10), biweekly, and a fourth/terminal dose a week later. Prior to each treatment and on sacrifice (week 24), pVL was determined. Within three subcutaneous doses of cARV NPs, a non-detectable pVL was established (week 19) and continued until week 22. After the establishment of a non-detectable pVL (week 19–22), 4 treated-mice were sacrificed for tissue drug concentration determination by LC-MS/MS analysis. A considerable amount of cARV was detected at the HIV-infection target and reservoir organs. Subsequently, pVL rebounded comparable to control group by week 24, (7 weeks post-terminal dosage). The present study demonstrated cARV NPs augments sustained ARV efficacy in the cHIV humanized-mouse model. Therefore, cARV NPs could be a novel delivery system to treat cHIV patients, by overcoming drawbacks of conventional cART.

*Corresponding author. Pharmacy Practice, Creighton University, 2500 California Plaza, Omaha, NE 68178, USA. Tel.: +1 402 280 2087; fax: +1 402 280 3320. SubhraMandal@creighton.edu (S. Mandal).

Conflict of interest

The authors do not have a commercial or other association that might pose a conflict of interest.

Appendix A. Supplementary data

Supplementary data related to this article can be found at http://dx.doi.org/10.1016/j.antiviral.2018.06.005.

Keywords

Combination antiretroviral drugs; Nanoparticles; HIV-1 treatment; Humanized mice model; Tenofovir alafenamide; Elvitegravir; Emtricitabine

1. Introduction

Globally, an estimated 37 million people are living with human immunodeficiency virus (HIV)-1 (UNAIDS, 2016). The Center for Disease Control and Prevention (CDC) 2014 report shows that in United States > 1.2 million people living with HIV and 13% are unaware of their status (UNAIDS, 2016). Joint United Nations Programme on HIV/AIDS (UNAIDS) reported use of antiretroviral drugs (ARVs) has resulted in approximately 45% reduction in death rate caused by HIV/Acquired Immune Deficiency Syndrome (HIV/AIDS), since 2004 (UNAIDS, 2016). However, HIV transmission rate is still unacceptably high. Internationally, the epidemic continues mainly due to high HIV transmission rate, patient non-adherence to ARVs, and lack of therapy access. A focus of developing novel effective long-acting parenteral therapeutics to improve the quality of life of HIV/AIDS infected people and to reduce the possibility of infection transmission (Mandal et al., 2017a).

We encapsulated tenofovir alafenamide, elvitegravir, and emtricitabine (TAF/EVG/FTC) into a polymeric nano-drug delivery system. To achieve long-acting drug delivery, poly (lactic-co-glycolic acid) (PLGA) (a FDA-approved polymer) was chosen for the ARVs nanoformulation, for its biocompatibility, biodegradability properties, and sustained release potential (Mandal et al., 2017b; Makadia and Siegel, 2011). The polymeric encapsulation of the ARV drugs demonstrates slow sustained release and limited systemic clearance (Mandal et al., 2017b). As cARV drugs, TAF/FTC/EVG combination were chosen without COBI, as PLGA polymer limits the systemic clearance of EVG and reported to provide hepatic P450 inhibition (Paolini et al., 2017). Based on the present study in the humanized mouse model, we report for the first time three cARV drugs encapsulated single nanoparticle (NP) formulation (i.e. TAF + EVG + FTC NPs) with the long-acting (LA) sustained cARV release potential, as a possible treatment module for chronic HIV patients.

2. Materials and methods

2.1. Materials

PLGA with 75:25 lactide:glycolide ratio (MW 4000–15,000), Poly (vinyl alcohol) (PVA) (M.W. 13,000–23,000), isoflurane, HEPES buffer and Phosphate Buffered Saline (PBS) were purchased from Sigma-Aldrich (St. Louis, MO, USA). Pluronic F127 (PF-127) was purchased from D-BASF (Edinburgh, UK) whereas TAF, EVG, and FTC (99% purity) were provided by Gilead Sciences Inc. (Foster City, CA, USA). Dextrose 5% in sterile water (D5W) was purchased from Baxter Heathcare Corp. (Chicago, IL, USA). Dimethyl sulfoxide (DMSO), trifluoroacetic acid (TFA), formic acid and acetonitrile were purchased from Fisher (Fair Lawn, NJ, USA). The IRDye® 800CW (IR) was purchased from LI-COR

Biosciences (Lincoln, NE, USA). All reagents were used as received without further purification.

2.2. Nanoparticle preparation and characterization

TAF, EVG and FTC loaded NPs (TAF + EVG + FTC NPs) and IR dye loaded NPs (IR NPs) were fabricated by water-in-oil-in-water (w-o-w) and oil-in-water (o-w) emulsion-solvent evaporation method respectively, following previously reported method with some modifications (Mandal et al., 2017a, 2017b). Briefly, for TAF + EVG + FTC NPs, FTC dissolved in 1 mM HEPES buffer (pH 9) was emulsified in DCM organic phase containing PLGA, PF127, and TAF + EVG (PLGA:PF127:TA-F:EVG:FTC at 1:1:0.7:0.5:0.5 ratio) obtaining water-in-oil (w-o) emulsion and sonicated. The above w-o emulsion was further emulsified in 1% PVA to obtained w-o-w emulsion and was sonicated obtaining TAF + EVG + FTC NPs. Moreover, IR NPs were obtained by emulsifying DCM organic phase containing IR, PLGA and PF127 (at 0.1:1:1 ratio), in 1% PVA aqueous phase and obtained o-w emulsion was sonicated to get IR NPs. In all cases, the excess surfactants and unbound drugs/dye were washed off from cARV NPs by dialysis (dialysis cassette, MWCO 20 kDa; Thermo Scientific, Waltham, MA, USA) with ultrapure water (18.2 MΩ cm). The NPs thus obtained were freeze-dried in the Millrock LD85 lyophilizer (Kingston, Fountain Valley, CA, USA).

The size, polydispersity index (PDI), and zeta potential of the NPs were characterized by using the ZetaPlus Zeta Potential Analyzer (Brookhaven Instruments Corp., Holtsville, NY, USA) (n = 4). To evaluate the percent encapsulation efficiency (% EE) of the cARVs in NPs, an aliquot of NPs were dissolved in DMSO, releasing the trapped ARV drug and analyzed using HPLC as described previously (Dinarvand et al., 2011; Mandal, 2016). The following equation was used to determined %EE:

$$\% EE = \frac{A_{NP}}{A_{initial}} \times 100$$

where, '$A_{initial}$' and 'A_{NP}' indicates the drug amount respectively added to the emulsion and entrapped in the NP.

2.3. In vivo bio-distribution studies in hu-NSG mice model

To follow *in vivo* bio-distribution of cARV NPs, the humanized NOD. Cg-Prkdc^{scid} I12rg^{tm1wjl}/SzJ, NSG (hu-NSG) mice were purchased from Jackson Laboratory (Bar Harbor, ME USA) for live animal imaging studies. After a week of acclimatization, hu-NSG mice (n = 3) received subcutaneously (SubQ) 22.8 mg/kg of IR as IR NPs in 0.5 mL D5W. At respective time points (1 h, 1, 8, and 14 days), mice were anaesthetized with isoflurane and live *in vivo* imaging (IVIS) was performed under *in vivo* Gamma camera (Kodak IS *in vivo* FX; Kodak, New Haven, CT USA). On 14th day, these mice were euthanized and the major organs of interest i.e., brain, female reproductive track (FRT), spleen, colon, and major lymph nodes were harvested and imaged to evaluate terminal tissue accumulation. The images were analyzed by using the Living Image 4.1 software and the data presents the epi-fluorescence intensity distribution has been expressed as photons/s/sr/cm^2.

2.4. Generation of hu-BLT mice

Hu-BLT mice were generated by following previously published protocols (Roncarolo and Carballido, 2001; Wang et al., 2014). Those hu-BLT mice that demonstrated human leukocytes to total leukocytes ratio greater than 50% in peripheral blood, were eligible for challenge with HIV-1 infection. At the end of the experiments, peripheral blood was obtained to determine percentage of human $CD4^+$ cells.

2.5. Ethics statement

All experiments on hu-NSG mice were adhered to the NIH Guide for the Care and Use of Laboratory Animals (Institutional Animal Care and Use Committee (Protocol #1059), University of Nebraska-Lincoln; UNL) and Creighton University (Protocol #0989) (Committee, 2015).

2.6. HIV-1 vaginal challenge and ARV NP administration

Female hu-BLT mice received intraperitoneally 2 mg of methox-yprogesterone 5 days before experiments commenced. Treatment and control mice received intravaginal dose (5×10^5 $TCID_{50}$ in 20 μL) of two HIV transmission/founder (T/F) viruses (WITO.c/2474 and SUMA. c/2821) from acutely infected patients (Fig. 2A). These infected-hu-BLT mice were maintained until week 15 to simulate chronic HIV infection and blood was drawn on week 15 post-inoculation (PI), to determine baseline plasma viral load (pVL) by RT-PCR. After 15th week blood draw, treated mice (n = 10) received subcutaneously (SubQ) mean dose of 417 mg/kg cARV as TAF + EVG + FTC NP in D5W. Control mice (n = 5) received equal volume of D5W SubQ (Fig. 2A). Above TAF + EVG + FTC NPs dosing was repeated biweekly for the first three doses. The biweekly dosing frequency was decided based on previously reported cARV NP single dose PK studies demonstrating non-detectable drug level by day 14 (Mandal et al., 2017b). For the same reason, all the treated mice received a terminal 4th dose 1 week after the 3rd dose. Further, mice were maintained and blood was collected biweekly for pVL, until pVL rebound back similar to infected-untreated-control mice. At the end of the study (week 24), the mice were sacrificed and blood was harvested for pVL estimation and to evaluate sustenance of humanized immune cells (human $CD4^+$ cells) by Flow cytometry.

2.7. Plasma viral load (pVL)

Viral RNA (vRNA) was extracted from the plasma obtained from treated and control mice using QIAamp Viral RNA Mini Kit (Qiagen, Valencia, CA, USA). To evaluate pVL, one-step RT-PCR analysis was performed using TaqMan® Fast Virus 1-Step Master Mix (ThermoScientific, Waltham, MA, USA) along with primers: forward 5′-GCCTCAATAAAGCTTGCCTTGA-3′, reverse 5′-GGGCGCCACTGCTA GAGA-3′ and a probe 5’-/FAM/CCAGAGTCACACAACAGACGGGCACA/BHQ_l/−3′ targeting the gag region of HIV-1. The RT-PCR cycle (45 cycle) was performed on an Applied Biosystems® 7500 Real-Time PCR Systems (ThermoScientific, Waltham, MA, USA). Data calculation and interpretation of fluorescence data was estimated by the RT-PCR instrument's software. Viral copy numbers of unknown samples were calculated from the regression equation obtained from standard curve obtained by plotting Ct-values against known viral copy

numbers (Li et al., 2005). All standards and unknown sample vRNAs were run in triplicate and duplicate, respectively. The detection limit of the assay was 800 copies per mL plasma.

2.8. Antiretroviral plasma and tissue retention analysis

Tissue samples from week 22 treated mice (n = 4), were analyzed for ARV concentration by following previously reported method (Prathipati et al., 2016). Briefly, 100 pL tissue homogenate (homogenized in deionized water [1:1 w/v] using beads) sample was mixed with 25 μL of internal standard spiking solution followed by 100 μL of 1% TFA addition. Samples were vortexed and extracted through solid-phase extraction cartridges. The eluent was evaporated to dryness under a stream of nitrogen, reconstituted with 100 μL of 50% acetonitrile-water and 5 μL was injected into the LC-MS/MS instrument. Chromatographic separation was carried out using a Restek Pinnacle DB Biph (2.1 mm × 50 mm, 5 μm) column with isocratic mobile phase consisting of 0.1% formic acid in water (A) and 0.1% formic acid in acetonitrile (B) (48:52 v/v) at a flow rate of 0.250 mL/min. The dynamic range of the validated assay was 1–2000 ng/mL for TFV, FTC and EVG.

An Exion HPLC system (Applied Biosystems, Foster City, CA, USA) coupled with AB Sciex API 5500 Q Trap with an electrospray ionization (ESI) source (Applied Biosystems, Foster City, CA, USA) operated in positive mode. The LC-MS/MS system was controlled by Analyst 1.6.1 software. Average inter-day and intra-day variability of the assay was < 15% according to the FDA analysis guidelines (Committee, 2013).

2.9. Statistical analysis

All vRNA copy numbers of unknown samples were estimated from the linear regression analysis of C_t values of the known standards viral copy numbers (log_{10}-transformed) [8]. All analyses were performed using the statistical software GraphPad Prism 7 (La Jolla, CA). The results were represented as mean ± standard error of means (SEM). The significant differences among treated and control groups at different time was considered to be statistically significant only at $p < 0.05$.

3. Results

3.1. Physicochemical characteristics of cARV NPs

The physicochemical characterization demonstrates TAF + EVG + FTC NPs were 243.2 ± 5.8 nm (mean ± SEM, n = 4) in size, uniformly spherical in morphology and monodispersed (PDI values < 0.2, a measure of NP size distribution pattern), and had negative surface charge of −20.73 ± 9.3 mV (Table 1) (Mandal et al., 2017a, 2017b). Estimated TAF, EVG and FTC % EE was 50.7 ± 2.6%, ± 2.9% and 46.4 ± 3.6%, respectively. Similarly, IR NP sized 203 ±13.2 (n = 3) with surface charge −27.6 ± 5.7 and ± 10.13% EE.

3.2. Bio-distribution and accumulation profile

The *in vivo* real-time bio-distribution and accumulation pattern of the cARV NPs was evaluated based on IR NPs (as cARV NPs surrogate) distribution over time (1 h, 1, 8 and 14 days) (Fig. 1). The IR NPs illustrated a uniformly distributed throughout the body within 1 h of SubQ injection (Fig. 1A). Over time (1 and 8 days), the IR NPs accumulation was

observed mainly near the lymphatic and vaginal area. Majorly, IR NPs accumulation was observed at the supraclavicular, axillary, inguinal and popliteal lymph node regions (Fig. 1A, dorsal image panel). Interestingly, all through the entire study, the injection site demonstrated a strong IR NP signal (Fig. 1, ventral image panel) suggesting NPs reside here and act as parenteral depot. Furthermore, at the end of the study (Day 14 post-injection) all the organs related to HIV-1 infection such as, infection sites (i.e. FRT and colon), the infection spread site (e.g. lymph nodes) and reservoirs such as spleen and brain, all showed significant amount of IR signal referring to IR NP accumulation in these areas (Fig. 1B, day 14 organ accumulation). Additionally, the presence substantial high IR fluorescent at the injection site and in the draining organs such as liver and kidney until on day 14 (supplementary Fig. 1) suggests injection site potentially induces gradual release of NPs and could be the contributing factor to sustained prolonged ARV presence when administrated as ARV NPs.

3.3. cARV NP treatment efficacy

To evaluate treatment efficacy of combined TAF + EVG + FTC NP, the *in vivo* treatment study design in humanized BLT mice was described (Fig. 2A). Baseline pVL (week 15, prior to cARV NP dosing) in treated mice averaged (± SEM) $3.5 \times 10^5 \pm 2.4 \times 10^5$ copies/mL and control mice $1.4 \times 10^6 \pm 8.0 \times 10^5$ copies/mL (Fig. 2B). The treated group pVL was significantly reduced to non-detectable levels by the 3rd dose (before 6th week) of cARV NPs SubQ treatment (administered biweekly), whereas as expected the control group resulted in high pVL of $2.4 \times 10^6 \pm 2.7 \times 10^5$ copies/mL. The mean non-detectable pVL was maintained until week 22 (2 weeks after the last dose). However, by week 24, the pVL rebounded to $2.5 \times 10^6 \pm 9.35 \times 10^5$, comparable to untreated control mice. Control mice pVL remained elevated throughout the experiment with the terminal vRNA load of $1.7 \times 10^6 \pm 7.9 \times 10^5$ copies/mL (Fig. 2B).

During the above study, when the pVL showed sustained non-detectable pVL (week 19–22), 4 mice were sacrificed on week 22 to obtain organs to determinate tissue drug concentrations by utilizing LC MS/MS methodology (Table 2). The observed mean (± SD) TFV, FTC, and EVG drug levels in lymph nodes were 333.4 ± 36.4, 87.7 ± 5.3, and 125.2 ± 49.3 ng/G, respectively. FRT tissue cART levels were 7.0 ± 1.5, 13.3 ± 10.1, and 13.2 ± 6.6 ng/G, respectively. Presence of detectable cARV tissues levels (lymph nodes and FRT) demonstrates that nano-encapsulation of cARV enhances drug permeability in privileged/infection prone tissues and confirms the sustained release properties from the polymeric NPs. Presence of cARVs in the draining organs such as liver and kidneys (Table 2) even two weeks after terminal dosing also supports long-acting potential of these polymeric NPs.

Finally, to confirm that hu-BLT continued to produce human CD4 cells over entire study-period; blood was obtained at week 15 and week 24 (study-terminal day) for flow cytometry to determine the percent human CD4 cells. For both control and treated groups the mean baseline human CD4 cells was > 80%. However, compared to week 12, a significant ($p < 0.0001$) reduction in the percent human CD4 cells was demonstrated at week 15 (control 45%, treated 35% treated groups). No significant difference in percent human CD4 cells from week 24 results was compared between the control and treated groups.

4. Discussion

A major focus of HIV treatment research is on the development of a long-acting injectable combination ARV (LAicARV). LAicARV for HIV treatment is getting popularity among patients living with HIV infection, as they need be on cARV treatment life-long. We proposed a novel cARV loaded nano-formulation composed of a biodegradable and biocompatible FDA-approved polymer to reduce safety risk. The PLGA polymer is a safe polymer as in endosomal it gets easily biodegrades into lactic and glycolic acid, which get utilized by body as metabolite of tricarboxylic acid cycle. The TAF, EVG and FTC drug are the three active ARVs combination along with cobicistat in the marketed Genvoya, product for HIV treatment (Department of Health and Human Services). We encapsulated these ARVs (except cobicistat) in the NP to induce a long-term sustained release phenomenon with the aim to overcome non-adherence without a prolonged sub-therapeutic tail that has been found with other long-acting nanoformulations (Landovitz et al., 2016).

Fabricated cARV NPs were of size < 250 nm with uniform distribution (PDI < 0.2) and having net low negative surface charge (Table 1). The size of the NPs was in the size range with reduced risk of causing clogging of the lymphatic ducts or fine capillaries (Bose et al., 2014; Zhang and Lu, 2014). Moreover, at the infection site due to inflammation, the gap between the lymphatic epithelial cells expands to 300–500 nm, promoting < 300 nm sized cARV NPs accumulation at the infected lymphatic areas (Dinarvand et al., 2011; Mandal, 2016). Additionally, neutral or low negative surface charge NPs sized < 250 nm have shown less cytotoxic (Bhattacharjee et al., 2010; Shao et al., 2015). We have previously reported that these cARV NPs were non-cytotoxic to various cell lines (Mandal et al., 2017a, 2017b).

Important advantages of an efficient drug carrier are their ability to whole-body bio-distribution and promote accumulation at the site of disease interest. The surrogate IR NP bio-distribution study reveals that within 1 h of SubQ injection, the NPs distributes uniformly all over the body and over time tends to accumulate at different tissues (Fig. 1). Another essential feature of next-generation nano-drug delivery system for systemic administration is establishment of local drug-depots (Mandal, 2016). The presence of substantially elevated IR fluorescence until the end of study (14 days post-injection) at the injection site and within clearance organs (liver and kidney) indicates at the injection site cARV NPs could act as a “cARV NP depo” inducing sustained NP release. The above observation follows the previous PK studies, reporting high cARVs concentration at the injection site and clearance organs at the terminal time-point (Prathipati et al., 2017).

For effective HIV suppression, local high ARV levels at the infection target site are needed. Bio-accumulation of surrogate IR NP at the HIV-1 infection associated organs such as lymph nodes, FRT, and colon showed high levels of IR accumulation, confirming our hypothesis that cARV NP encapsulation prolongs cARV-retention (Fig. 1B). Previous PK studies suggested that subQ injected cARV NP leads to ARVs target tissue-level significantly above the IC_{90} (Mandal et al., 2017a, 2017b; Prathipati et al., 2017) for all three studied ARVs. Compared to single cARV PK studies (Mandal et al., 2017a, 2017b; Prathipati et al., 2017), multiple dosage of cARV NPs illustrated even higher tissue ARV levels at 22 week (2 weeks post-terminal dose, Table 2). Further, sustained non-detectable

pVL (Fig. 2B), further supports the cARV NP release due to NP polymer slow endosomal-degradation induces steady cARV release and enhances local high cARV levels over a prolonged period essentially for HIV suppression (Shao et al., 2015; Baluk et al., 2007; Cueni and Detmar, 2006; Petushkov et al., 2009). Moreover, cARV NP PK study report also established that cARV concentration significantly subsides by day 14 post-treatment, which explicitly explains the cause of pVL rebound 4 weeks after terminal 4th dosage (Fig. 2B).

The LATTE-2 study demonstrated cabotegravir (CAB) and rilpivirine (RPV) loaded LAiARV nanosuspension administrated intramuscular at intervals once monthly or biweekly was as effective as daily oral intake of CAB with two NRTIs (Margolis et al., 2017). The dosage studied was 400 mg CAB + 600 mg RPV monthly or 600 mg CAB + 900 mg RPV bimonthly. After 96 weeks, 94% and 95% patients respectively of once monthly and bimonthly treatment regimen showed non-detectable pVL. The present TAF + EVG + FTC NP formulation was administered SubQ biweekly at 139 mg/kg dosage of each drug (all together cARV dosage was 417 mg/kg) to the chronically infected HIV-1 hu-BLT mice. The study demonstrates that within 3 doses of cARV NPs treatment (i.e. 6 weeks post-1st treatment), the pVL of the treated group decreased to non-detectable levels and significantly suppressing pVL compared to untreated-infected control group (Fig. 2B). Furthermore, the non-detectable pVL was maintained for 3 consecutive weeks from week 19 until 22 (post HIV-1 infection) and 2 weeks after last dosage of cARV NP treatment (Fig. 2B). Control mice demonstrated elevated pVL throughout the experiment, ending at $1.7 \times 10^6 \pm 7.9 \times 10^5$ copies/mL.

Other investigators have also reported efficacy of using LA ARV nanoformulations in mouse models for acute HIV (Roy et al., 2012; Jiang et al., 2015; Puligujja et al., 2015), and in macaques or human phase II trial for chronic HIV infection (Roy et al., 2012; Shao et al., 2016; Markowitz et al., 2017; Margolis et al., 2015). However, present study is the first report to formulate three ARVs loaded LA NPs to treat chronically HIV infected humanized mouse model, closely mimics cARV dosing used for treating HIV patients. Considering, basal metabolic rate (kcal/day) of mouse is approximately seven-times higher than human (Perlman, 2016) and based on FDA supported allometric exponent of 0.75 (Guidance for Industry, 2015), we hypothesize that cARV nano-encapsulation could significantly reduce dosing frequency from daily to monthly for human use. Our next aim is to evaluate LAicARV potentially of present nano-formulation in non-primate model.

In conclusion, present studies demonstrate that cARV NPs prove to be a potent, LAicARV nano-system at the humanized animal model to treat chronic HIV-1. This is the first proof-of-concept report of the following three cARV loaded NP (TAF + EVG + FTC NP) of U.S. Department of Health and Human Service regimen that demonstrates pVL suppression to non-detectable levels at within three doses of biweekly SubQ administration.

Supplementary Material

Refer to Web version on PubMed Central for supplementary material.

Acknowledgements

The authors wish to thank Gilead Sciences, Inc. and James Rooney, M. D., for their gift of the TAF, EVG, and FTC drug powders. Authors are thankful to Prof. Tu, Department of Pharmacology, Creighton University, for his generous help in performing IVIS imaging study. Present work and publication has been funded by NIAID R01AI117740-01, 2015 (to C.J.D.). This manuscript has been presented in part at the 2016 ASM-Microbe Conference, Boston, MA June 16–20 as a poster. (abstract #16-1812).

Abbreviations

LA	Long-acting
cARVs	Combination antiretroviral drugs
cHIV	Chronic HIV-1
hu-BLT	Humanized-BLT
pVL	Plasma viral load
PLGA	Poly (lactic-co-glycolic acid)
PVA	Poly (vinyl alcohol)
PF-127	Pluronic F127
D5W	Dextrose 5%
DMSO	Dimethyl sulfoxide
TFA	Trifluoroacetic acid
IR	IRDye® 800CW
hu-NSG	Humanized NOD.Cg-PrkdcscidIL2rgtm1Wjl/Szj
FRT	Female reproductive track
T/F	HIV transmission/founder
pVL	Plasma viral load
vRNA	Viral RNA
LAicARV	Long-acting injectable combination ARV

References

Baluk P, Fuxe J, Hashizume H, Romano T, Lashnits E, Butz S, et al., 2007 Functionally specialized junctions between endothelial cells of lymphatic vessels. J. Exp. Med 204 (10), 2349–2362. [PubMed: 17846148]

Bhattacharjee S, de Haan LHJ, Evers NM, Jiang X, Marcelis ATM, Zuilhof H, et al., 2010 Role of surface charge and oxidative stress in cytotoxicity of organic monolayer-coated silicon nanoparticles towards macrophage NR8383 cells. Part. Fibre Toxicol 7 (1), 25. [PubMed: 20831820]

Bose T, Latawiec D, Mondal PP, Mandal S, 2014 Overview of nano-drugs characteristics for clinical application: the journey from the entry to the exit point. J. Nanoparticle Res 16 (8), 2527.

Committee, 2013 Guidance for Industry: bioanalytical method validation In: Services USDoHaH. Food and Drug Administration, Rockville, MD, USA.

Committee, 2015 Guide for the Care and Use of Laboratory Animals 8 Ed. Council GBotNR. The National Academies Press, Washington, DC, USA.

Cueni LN, Detmar M, 2006 New insights into the molecular control of the lymphatic vascular system and its role in disease. J. Invest. Dermatol 126 (10), 2167–2177. Department of Health and Human Services, Website: https://aidsinfo.nih.gov/drugs/507/stribild/0/patient. [PubMed: 16983326]

Dinarvand R, Sepehri N, Manoochehri S, Rouhani H, Atyabi F, 2011 Polylactide-co-glycolide nanoparticles for controlled delivery of anticancer agents. Int. J. Nanomed 6, 877–895.

Guidance for Industry, 2015 Estimating the Maximum Safe Starting Dose in Initial Clinical Trials for Therapeutics in Adult Healthy Volunteers.

Jiang Y, Cao S, Bright DK, Bever AM, Blakney AK, Suydam IT, et al., 2015 Nanoparticle-based ARV drug combinations for synergistic inhibition of cell-free and cell-cell HIV transmission. Mol. Pharm 12 (12), 4363–4374 [PubMed: 26529558]

Landovitz RJ, Kofron R, McCauley M, 2016 The promise and pitfalls of long-acting injectable agents for HIV prevention. Curr. Opin. HIV AIDS 11 (1), 122–128. [PubMed: 26633643]

Li Q, Duan L, Estes JD, Ma ZM, Rourke T, Wang Y, et al., 2005 Peak SIV replication in resting memory CD4+ T cells depletes gut lamina propria CD4+ T cells. Nature 434 (7037), 1148–1152. [PubMed: 15793562]

Makadia HK, Siegel SJ, 2011 Poly lactic-co-glycolic acid (PLGA) as biodegradable controlled drug delivery Carrier. Polymers 3 (3), 1377–1397. [PubMed: 22577513]

Mandal S, 2016 Multimodal nanosystem: the future medicine. iScience Notes 1 (1).

Mandal S, Belshan M, Holec A, Zhou Y, Destache CJ, 2017a An enhanced emtricitabine-loaded long-acting nanoformulation for prevention or treatment of HIV infection. Antimicrob. Agents Chemother. 61 (1).

Mandal S, Prathipati PK, Kang G, Zhou Y, Yuan Z, Fan W, et al., 2017b Tenofovir alafenamide and elvitegravir loaded nanoparticles for long-acting prevention of HIV-1 vaginal transmission. AIDS 31 (4), 469–476. [PubMed: 28121666]

Margolis DA, Brinson CC, Smith GHR, de Vente J, Hagins DP, Eron JJ, et al., 2015 Cabotegravir plus rilpivirine, once a day, after induction with cabotegravir plus nucleoside reverse transcriptase inhibitors in antiretroviral-naive adults with HIV-1 infection (LATTE): a randomised, phase 2b, dose-ranging trial. Lancet Infect. Dis. 15 (10), 1145–1155. [PubMed: 26201299]

Margolis DA, Gonzalez-Garcia J, Stellbrink HJ, Eron JJ, Yazdanpanah Y, Podzamczer D, et al., 2017 Long-acting intramuscular cabotegravir and rilpivirine in adults with HIV-1 infection (LATTE-2): 96-week results of a randomised, open-label, phase 2b, non-inferiority trial. Lancet 390 (10101), 1499–1510. [PubMed: 28750935]

Markowitz M, Frank I, Grant RM, Mayer KH, Elion R, Goldstein D, et al., 2017 Safety and tolerability of long-acting cabotegravir injections in HIV-uninfected men (ECLAIR): a multicentre, double-blind, randomised, placebo-controlled, phase 2a trial. Lancet HIV 4 (8), e331–e340. [PubMed: 28546090]

Paolini M, Poul L, Berjaud C, Germain M, Darmon A, Bergere M, et al., 2017 Nano-sized cytochrome P450 3A4 inhibitors to block hepatic metabolism of docetaxel. Int. J. Nanomed 12, 5537–5556.

Perlman RL, 2016 Mouse models of human diseaseAn evolutionary perspective. Evol. Med. Publ. Health 2016 (1), 170–176.

Petushkov A, Intra J, Graham JB, Larsen SC, Salem AK, 2009 Effect of crystal size and surface functionalization on the cytotoxicity of silicalite-1 nanoparticles. Chem. Res. Toxicol 22 (7), 1359–1368. [PubMed: 19580308]

Prathipati PK, Mandal S, Destache CJ, 2016 Simultaneous quantification of tenofovir, emtricitabine, rilpivirine, elvitegravir and dolutegravir in mouse biological matrices by LC-MS/MS and its application to a pharmacokinetic study. J. Pharmaceut. Biomed. Anal 129, 473–481.

Prathipati PK, Mandal S, Pon G, Vivekanandan R, Destache CJ, 2017 Pharmacokinetic and tissue distribution profile of long acting tenofovir alafenamide and elvitegravir loaded nanoparticles in humanized mice model. Pharm. Res. (N. Y.) 34 (12), 2749–2755.

Puligujja P, Arainga M, Dash P, Palandri D, Mosley RL, Gorantla S, et al., 2015 Pharmacodynamics of folic acid receptor targeted antiretroviral nanotherapy in HIV-1-infected humanized mice. Antivir. Res 120, 85–88. [PubMed: 26026666]

Roncarolo MG, Carballido JM, 2001 Construction of human-SCID chimeric mice Curr. Protoc. Im Chapter 4: Unit 4.8 .

Roy U, McMillan J, Alnouti Y, Gautum N, Smith N, Balkundi S, et al., 2012 Pharmacodynamic and antiretroviral activities of combination nanoformulated antiretrovirals in HIV-1-infected human peripheral blood lymphocyte-reconstituted mice. J. Infect. Dis 206 (10), 1577–1588. [PubMed: 22811299]

Shao XR, Wei XQ, Song X, Hao LY, Cai XX, Zhang ZR, et al., 2015 Independent effect of polymeric nanoparticle zeta potential/surface charge, on their cytotoxicity and affinity to cells. Cell Prolif 48 (4), 465–474. [PubMed: 26017818]

Shao J, Kraft JC, Li B, Yu J, Freeling J, Koehn J, et al., 2016 Nanodrug formulations to enhance HIV drug exposure in lymphoid tissues and cells: clinical significance and potential impact on treatment and eradication of HIV/AIDS. Nanomedicine 11 (5), 545–564. [PubMed: 26892323]

(UNAIDS) JUNPoHA, 2016 GLOBAL HIV STATISTICS. Factsheet- World AIDS Day 2017: Communications and Global Advocacy.

Wang LX, Kang G, Kumar P, Lu W, Li Y, Zhou Y, et al., 2014 Humanized-BLT mouse model of Kaposi's sarcoma-associated herpesvirus infection. Proc. Natl. Acad. Sci. U. S. A 111 (8), 3146–3151. [PubMed: 24516154]

Zhang XY, Lu WY, 2014 Recent advances in lymphatic targeted drug delivery system for tumor metastasis. Cancer Biol Med 11 (4), 247–254. [PubMed: 25610710]

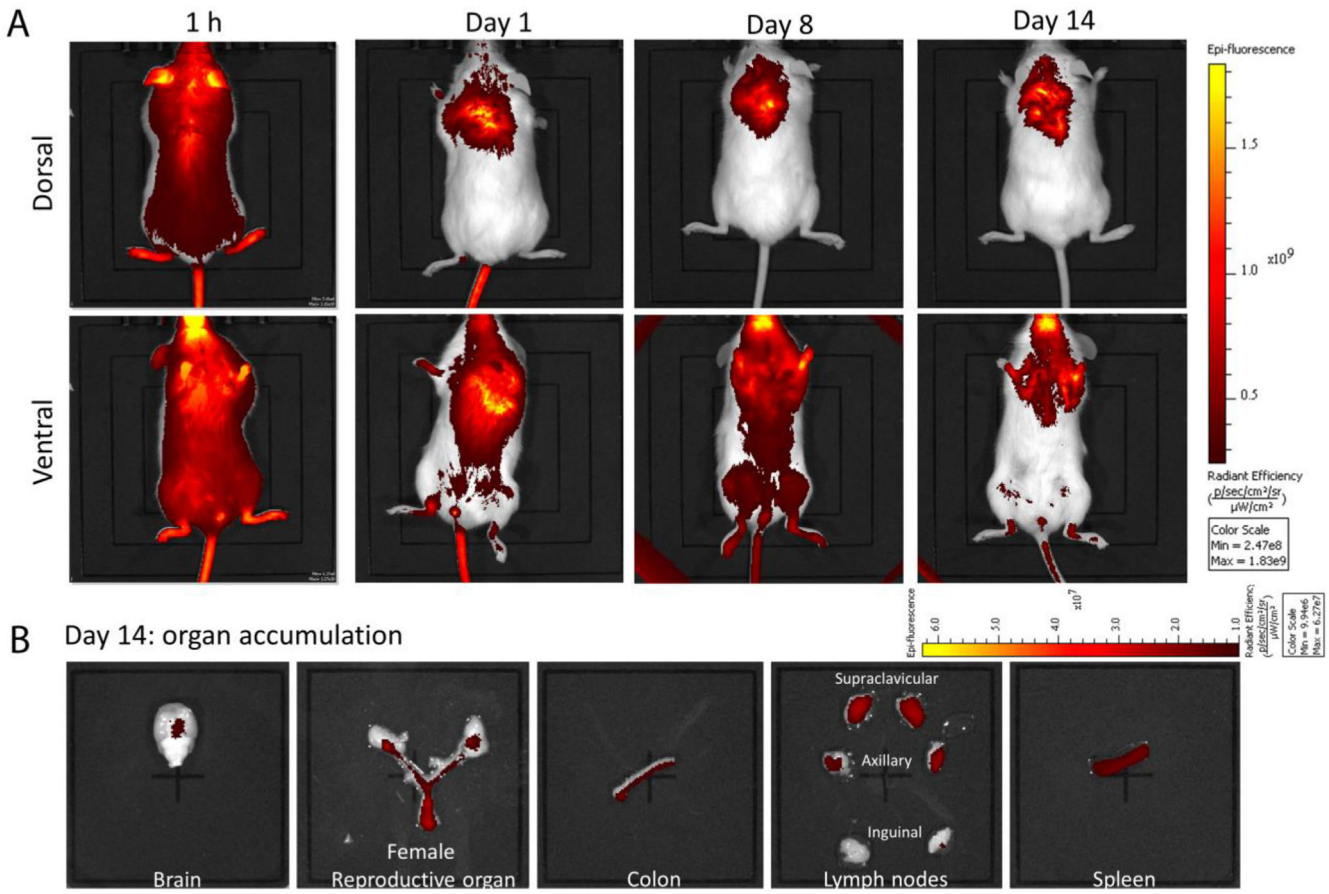

Fig. 1.

Bio-distribution and bio-accumulation study of IR NPs. A) Live animal images illustration bio-distribution profile of IR NP. Representative images of 1 h, day 1, 8 and 14 are shown. Upper panel represents ventral side of mice and the lower panel represents dorsal side of mice. B) Target organ accumulation profile of IR NP at end of experiment (day 14). The images are representative IR accumulation in brain, female reproductive tract, colon, lymph nodes, and spleen. All images were obtained with constant specifications i.e., excitation filter: 745 nm; emission filter: Open; fluorescent level: low (for time 1 h, 8 h and day 1) and high (for day 8 and 16); exposure time: 1 s. The entire image scale bar represents epi-fluorescence intensity as radiation intensity.

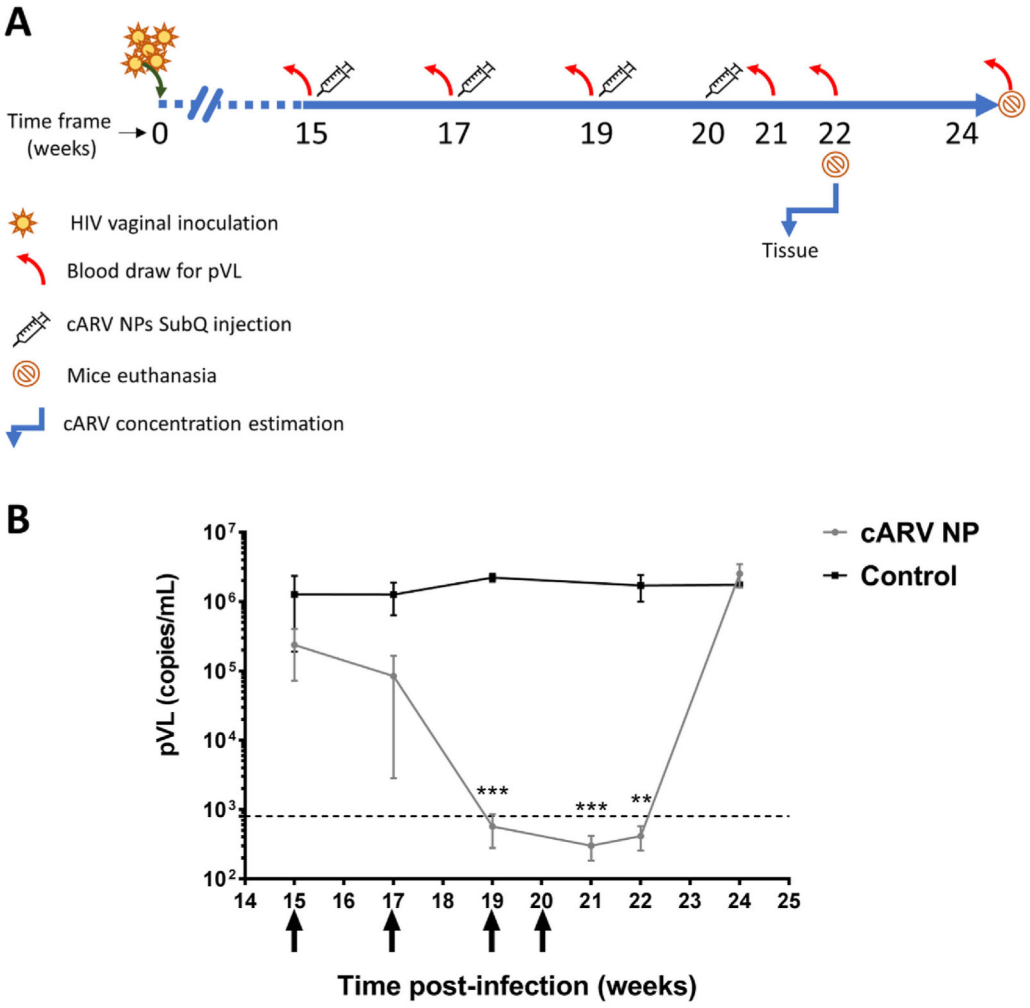

Fig. 2.

Plasma viral load (pVL) comparison in hu-BLT mice that received treatment (n = 10) and control (n = 5). A) Schematic presentation of the treatment study design. B) Graphical presentation of pVL data over entire study period. Four doses (black arrows below X-axis) show when ARV NPs were administered (every 2 weeks (Landovitz et al., 2016; Bose et al., 2014; Zhang and Lu, 2014) and final dose administered on week 20). Hu-BLT mice received a mean 417 mg/kg cARV NPs as a total dose. Treated group pVL was significantly reduced (** and *** represents $p \leq 0.01$ and 0.001, respectively) compared to control group.

Table 1

Physicochemical characteristics of TAF+EVG NPs and FTC NPs.

ARV NP type	Size (nm)*	Polydispersity index (PDI)*	Surface Charge (mV)*	% Entrapment Efficiency (% EE)*
TAF + EVG + FTC NP	243.2 ± 5.8	0.130 ± 0.0035	−26.9 ± 1.8	TAF: 50.8 ± 2.6 EVG: 38.6 ± 2.9 FTC: 46.4 ± 3.6
IR NP#	203 ± 13.2	0.134 ± 0.036	−27.69 ± 5.7	70.7 ± 10.13

*n = 4 independent batches

#*n = 3 independent batches; Data presents mean ± Standard Error (SEM).* NP = nanoparticle; TAF+EVG = tenofovir alafenamide + elvitegravir; FTC = emtricitabine; IR = infra-red dye.

Antiviral Res. Author manuscript; available in PMC 2020 May 15.

Table 2

Tissue cARV drug concentration on week 22 (post HIV-infection).

Tissue type	Drug concentration (ng/G)		
	TFV	EVG	FTC
Lymph Node	333.43 ± 36.35	125.18 ± 49.27	87.74 ± 5.26
Spleen	BLQ	2.92 ± 0.97	16.27 ± 7.25
FRT	7.04 ± 1.49	13.23 ± 6.59	13.31 ± 10.11
Liver	38.91 ± 29.96	8.45 ± 4.34	15.96 ± 2.95
Kidney	BLQ	10.48 ± 1.47	25.41 ± 8.02

n = 4; Data presents mean ± standard deviation (SD); BLQ = Below limit of quantification; EVG = Elvitegravir; FRT = Female reproductive tract; FTC = Emtricitabine; TFV = Tenofovir.